

2022

## Friction Stir Welding of Polycarbonate Butt-Joint: Defects and Remedies

Mohamed Abdelmohsen Omer

Follow this and additional works at: <https://digitalcommons.aaru.edu.jo/erjeng>

---

### Recommended Citation

Abdelmohsen Omer, Mohamed (2022) "Friction Stir Welding of Polycarbonate Butt-Joint: Defects and Remedies," *Journal of Engineering Research*: Vol. 6: Iss. 2, Article 9.  
Available at: <https://digitalcommons.aaru.edu.jo/erjeng/vol6/iss2/9>

This Article is brought to you for free and open access by Arab Journals Platform. It has been accepted for inclusion in Journal of Engineering Research by an authorized editor. The journal is hosted on [Digital Commons](#), an Elsevier platform. For more information, please contact [rakan@aar.edu.jo](mailto:rakan@aar.edu.jo), [marah@aar.edu.jo](mailto:marah@aar.edu.jo), [u.murad@aar.edu.jo](mailto:u.murad@aar.edu.jo).

# Friction Stir Welding of Polycarbonate Butt-Joint: Defects and Remedies

Mohamed A. E. Omer<sup>1</sup>, Ezzat A. Showaib<sup>1</sup>, Maher Rashad<sup>1</sup>

<sup>1</sup>Department of Production Engineering and Mechanical Design, Tanta University, Tanta, 31527, Egypt

# Corresponding author email: [moh.mohsen95@f-eng.tanta.edu.eg](mailto:moh.mohsen95@f-eng.tanta.edu.eg)

**Abstract:** Friction stir welding (FSW) was initially developed for welding aluminium alloys which were difficult to weld using conventional welding techniques. With the remarkable success accomplished with these alloys, materials manufacturers were passionate about using FSW with other materials. In the case of polymeric materials, the application of conventional FSW was not satisfactory due to the differences between the characteristics of metals and polymeric materials. Consequently, many modifications were developed to overcome the drawbacks of conventional FSW technique. For instance, heating the tool with an external heating source is one of the major modifications. The aim of this work is to clarify the quality of friction stir welding of polycarbonate (PC) in square butt configuration as a function of tool temperature, rotational speed and welding speed. This material was selected due to its transparency as well as its good photoelastic properties. Therefore, the defects can be easily detected and the residual stresses can be revealed under a polarized optical microscope. Four values of suggested welding parameters (pin temperature, rotational speed and welding speed) were investigated. Both the mechanical properties and the defect formation were studied in order to achieve a better welding joint. The investigation of samples macrostructure showed that several defects such as islands of melted and non-melted material, discontinuous bonding line, macro-cracks, tunnels, flash formation, surface grooves, voids and root defects were formed as a response to the different interactions between the welding parameters. These defects can be minimized when the welding process is performed at a rotational speed of 1800 rpm, welding speed of 30 mm/min and tool temperature of 50°C. In this situation, the joint efficiency of the welded joint reached 92.2% relative to the base material flexural strength.

**Keywords:** Friction stir welding; Welding defects; Thermoplastic welding; Permanent joints; Induction heating; Friction welding

## 1 INTRODUCTION

Usage of polymeric materials in various industries, such as electronics, aviation, automotive, construction and packaging has increased because of their low weight, high specific strength, design flexibility, recyclability and low manufacturing cost. The increasing use of polymeric materials leads to a considerable increase in all related production processes. Due to the production of large and complex parts, joining process became one of the major processes performed during the production of these parts [1]. Mechanical fastening, bonding and welding are the essential methods to join thermoplastic parts together. In general, mechanical fasteners such as rivets and screws require the plastic parts to be strong enough to endure the strain of fastener insertion and subsequent stress concentration around the holes [2].

On the other hand, solvent and adhesive bonding is not appropriate in large scale production due to the long-time needed to produce a full joint strength [3]. With respect to welding processes, FSW is a promising technique for joining thermoplastic materials. In 1991, Wayne Thomas et al. [4] invented the FSW process at The Welding Institute (TWI, Cambridge, UK) for the purpose of welding high-strength aluminum alloys, which are classified as difficult to weld material via conventional techniques. FSW is performed using a non-consumable rotating tool which rotates around its own axis and moves along the welding path [5]. After welding the desired distance, the FSW tool is retracted from the welded plates leaving a key-hole at the end of the welding path.

The rotational direction of the welding tool and traversing direction of the material being welded divided the stir zone into advancing and retreating sides as shown in Fig. 1. In case the linear velocity of the rotational tool and the traverse movement of the workpiece have the same direction, the welding area is considered as the advancing side (AS). While the retreating side (RS) is formed in the area where these two velocities are contradicting each other. Previous studies concluded that the lack of bonding has mainly occurred at RS due to the poor mixing of materials at this area. Mendes et al. [6] welded Acrylonitrile Butadiene Styrene (ABS) using a stationary shoulder and concluded that a significant decrease in the cavities formed in RS can be achieved by applying sufficient axial force and high rotational speed. Kumar and Roy [7] investigate the possibility of joining glass-filled Nylon 6 composites using a cylindrical FSW pin profile under three values of rotational speed (300, 600 and 900 rpm) and tool traverse speed (0.1, 0.2 and 0.3 mm/s). A joint efficiency corresponding to 51.32 % relative to base material tensile strength was obtained. In addition, flaws such as tunnel defects, cracks, pores and wormholes were found in the weld nugget of the samples welded at the lowest value of rotational speed and the highest value of traverse speed.

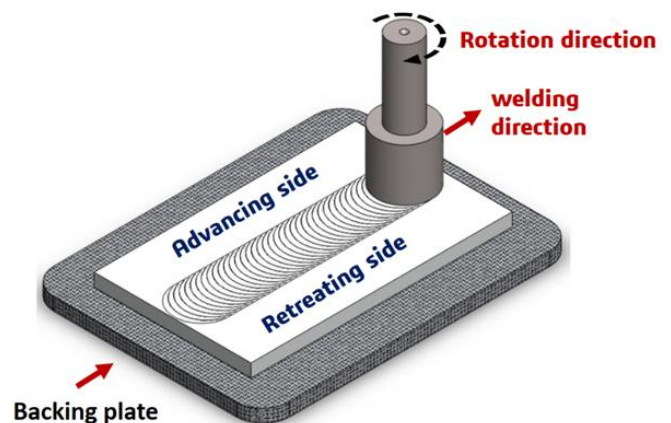


Fig. 1 Schematic illustration of FSW process.

Nath et al. [8] joined a 3 mm thick polypropylene (PP) sheet via a new self-heated FSW tool to investigate the effect of four values of rotational speed (1400, 1500, 1600 and 1700 rpm) on the tool force, spindle torque, joint microstructure and micro-hardness. During experimentation, a tool tilt angle of  $1^\circ$  and welding speed of 0.3 mm/s were kept at the mentioned values. Based on the obtained results, decreasing the tool rotational speed leads to increasing the amount of micro-voids as well as increasing the micro-hardness. Whereas the tool force and spindle torque decrease when the tool rotational speed increases. Sahu et al. [9] studied the effect of three different tool pin profiles (conical pin, square pin and cylindrical pin) on welding of 6 mm PP sheets under three values of rotational speed and welding speed. During all experiments, the material peeling defect (plastic tiny particles resemble chips in machining process) was observed over the plates surface due to the shoulder rubbing.

Rehman et al. [10] studied the influence of bottom preheating, rotational speed and welding speed on the joint efficiency during FSW of 6 mm thick high-density polyethylene (HDPE). They concluded that the strength of the welded joint can be increased by increasing the preheating temperature and rotational speed. They also mentioned that the failure of almost all tensile specimens started from the region of root defect. Eslami et al. [11] concluded that, it is challenging to produce a defect-free weld due to the existence of root defect. However, in order to prevent such a defect, the process parameters are required to be set at the values that generate a high welding temperature.

Sheikh-Ahmad et al. [12] examined the material flow patterns during FSW of HDPE sheets (one sheet has a white color whereas the second sheet has a black color) were also investigated. It was found that most of the welding defects are concentrated at the bottom area of the welding nugget where the heat is not sufficient to fuse the two parts together. In addition, the process temperature was found to have a prominent effect on the extent of material flow which in consequence affects the formation of defects. This study was held in an effort to comprehend the various types of defect formation and their causes during FSW of polycarbonate. The details about the raw material, equipment, process preparation and test procedure are represented. This is followed by a representation of the joints' mechanical properties that were produced based on Taguchi L16 orthogonal array. Then, the welding appearance was analyzed and the distribution of defects across the welded samples are listed. Finally, the cross-section of the welded samples was grouped according to their relevance in terms of the type of defect and discussed in detail.

## 2 EXPERIMENTAL PROCEDURE

In this research work, FSW experiments were carried out on commercial 6 mm PC plates which were manufactured by ‘‘Polyee Plast Factory’’ in Bader city, Egypt. Typical properties of PC are

listed in Table 1 as provided by the manufacturer. The specimens were cut into the dimensions of 90 mm x 120 mm using a disc milling. Polycarbonate is a naturally transparent amorphous polymer. The versatile characteristics of PC such as high dimensional stability, high impact-resistance, transparency, UV-protection, sound insulation, flame resistance and recyclability make it used in a wide range of industries including electronics, constructions, Automobile, aircraft, and railway. the welding procedure was performed in a single pass along x-axis using a customized 3-axis FSW machine (Fig. 2), this machine was described elsewhere [13].

Due to the preference for a stationary shoulder over a rotating one during welding of thermoplastic materials, the shoulder was fixed with the machine head using two rotational blockers. In order to heat the FSW tool (the FSW probe is a threaded cylindrical (M6) with a 5.5 mm effective length.) with an external heating source, an induction heating system has been used. The induction heating board was mounted on the machine head and the induction copper coil is placed concentric around the tool as shown in Fig. 2. For the purpose of controlling the probe temperature, a K-type thermocouple was inserted inside the stationary shoulder. During calibration, the temperature of the measured location was found to be lower than the FSW probe by about  $3^\circ\text{C}$ .

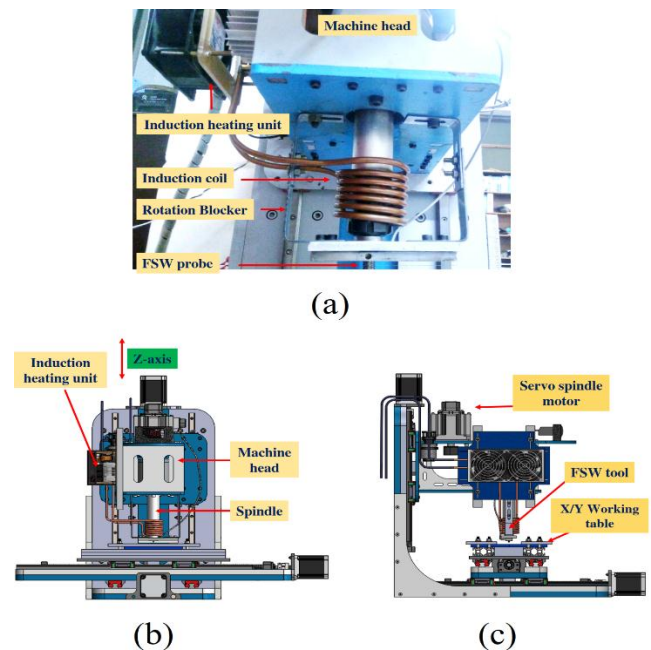


Fig. 2 The friction stir welding machine: (a) experimental setup, (b) machine front view and (c) machine side view

Table 1: Specifications of PC sheets.

Characteristic	Unit	Value
Light transmission	%	88-92
Specific gravity	$\text{g}/\text{cm}^3$	1.2
Coefficient of thermal expansion	$\text{mm}/\text{m } ^\circ\text{C}$	0.065
Heat conductivity	$\text{W}/\text{m}^2 \text{ } ^\circ\text{C}$	0.21
Tensile strength	MPa	$\geq 60$
Flexural strength	MPa	92.8
Modulus of elasticity	MPa	2154
Tensile strength at break	MPa	$\geq 65$

## 2.1 Process preparation

In order to determine the experimental domain of the process parameters, a number of stir-in-plate welding trials was conducted on PC sheets. The preliminary experimental plan included a wide range of welding speed (from 10 up to 150 mm/min), rotational speed (100 up to 1800 rpm) and tool temperature (from 50 up to 200 °C) while the spindle direction, pin geometry, shoulder size and plunging depth were kept without change. Based on the results of stir-in-plate welding, three values of welding speed, rotational speed and tool temperature were selected as represented in Table 2. In each experiment, the reference point (entry point) was adjusted by touching the bottom surface of the shoulder to the upper surface of the PC sheets with the guarantee of making the tool probe exactly between the plastic plates. After welding, the results were assessed according to a visual and macrostructure investigation.

## 2.2 Test procedure

In order to determine the mechanical properties of the welded joints, test specimens were extracted from the welded plates using a circular saw with a toothed disc according to ASTM D790 standard (Flexural Properties of Unreinforced and Reinforced Plastics and Electrical Insulating Materials) [14]. During cutting, the place being cut was water-cooled in order to prevent the specimens from the effect of overheating. In addition, a thin section from the welded plate was also prepared using tooth less circular saw. This thin section was used to investigate the weld zone using both optical stereo and transmission polarized microscope. Figure 3 shows examples of the tested samples and thin section locations.

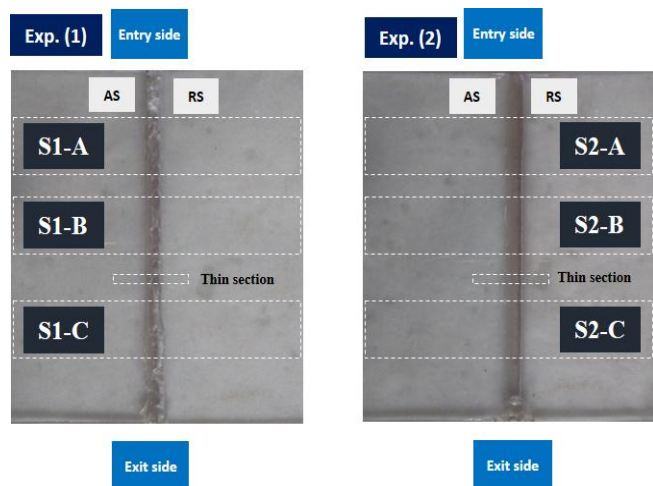


Fig. 3 Overall views of the square butt welded joints as well as the location of the tested samples and thin section for experiments parameters number 1 and 2 (Where S stands for sample). These are just 2 examples out of the 16 experiments to show the location of tested samples.

The test specimens were subjected to a three-point bending (according to the same aforementioned ASTM standard [14]); two supports carry the test sample and a load is applied with a single point using a loading nose moving at a constant rate in the centerline of the sample. The support span has to be 16 times the sheet thickness (96 mm in this case) and the rate of crosshead speed was set at 2.56 mm/min, which calculated using the following formula:

$$R = \frac{ZL^2}{6d} \quad (1)$$

where R is the rate of crosshead speed (mm/min), L is length of span (96mm), d is the depth of specimen (6mm), and Z is the rate of straining of the outer fibre (mm/min), Z has to be equal to 0.01. During performing the test, the machine is plotting and recording the simultaneous load-deflection data and the corresponding flexural stress and flexural strain were calculated by applying the following formulas:

$$\sigma_f = \frac{3PL}{2bd^2} \quad (2)$$

$$\epsilon_f = \frac{6Dd}{L^2} \quad (3)$$

where  $\sigma_f$  is the stress in the outer fibres at mid-point (MPa), P is the load (N), b is the width of specimen tested (mm),  $\epsilon_f$  is the *strain* in the outer surface (dimensionless quantity), and D is the maximum deflection of the midpoint of the test specimen (mm).

Table 2: Welding parameters and their values.

Welding parameter	Symbol/unit	Values
Welding speed	V (mm/min)	30, 60, 90 and 120
Rotational speed	N (rpm)	700, 1200, 1500 and 1800
Tool temperature	T (°C)	50, 90, 120 and 140

## 3 RESULTS AND DISCUSSIONS

### 3.1 Mechanical properties of the welded joints

The experimental plan was designed based on Taguchi L16 orthogonal array along with the relative flexural strength is represented in Table 3. Sample 12 which was joined at a welding speed of 90 mm/min, a rotational speed of 1200 rpm and tool temperature of 90 °C achieved the highest flexural strength (75 MPa) which corresponding to 80.8% compared with base material. On the other hand, the minimum relative flexural strength (about 35.4% and 35.9%) occurred in the samples welded in experiment number 1 and 13, respectively.

In the case of sample 1, the sample was joined at the minimum value of travel speed, rotational speed and tool temperature. These conditions did not allow the two pieces to stir properly due to the low rotational speed and the lack of heat. In the case of sample 13, the two pieces were joined at one of the worst parameter mixtures which is the minimum value of rotational speed and the maximum value of both welding speed and tool temperature.

### 3.2 Welding appearance of the square butt welded plates

The surface appearance of the welded samples should satisfy the required value of quality because it has importance from the commercial point of view. Simultaneously, surface appearance can be used as an initial tool to assess the welding quality during the preliminary welding trials. For instance, the amount of flash or chips along the welding line has an indication of internal defects such as porosities, cavities and tunnel defects. On the other hand, achieving an acceptable relative joint strength without taking the surface appearance into account at the design stage involving the welding setup and choosing the right set of parameters will increase the cost per unit.

**Table 3: Taguchi L16 orthogonal array and the mean of flexural strength.**

Exp./ Sample number	v (mm/min)	N (rpm)	T (°C)	$\sigma_f$ (MPa)	Joint efficiency (%)
1	30	700	50	32.9	35.4
2	30	1200	90	60.6	65.3
3	30	1500	120	46	49.5
4	30	1800	140	50.9	54.9
5	60	700	90	41.1	44.3
6	60	1200	50	55.2	59.5
7	60	1500	140	61.6	66.4
8	60	1800	120	70.1	75.6
9	90	700	120	64.5	69.5
10	90	1200	140	60.3	64.9
11	90	1500	50	65.9	71.0
12	90	1800	90	75.0	80.8
13	120	700	140	33.4	35.9
14	120	1200	120	50.4	54.3
15	120	1500	90	54.5	58.8
16	120	1800	50	44.9	48.4
Base	-	-	-	92.8	100

appearance of sample 1 and 5 have the same look which resembles a series of rope knots. These samples were welded at the lowest welding speed (700 rpm). The number of rope knots in sample 5 and its consistency is much higher than that in sample 1.

It is believed that was resulting from the variation of tool temperature and welding speed. This variation made sample 5 melted with a higher degree and that can be seen from the flash color around the welding line. The samples joined at a welding speed of 30 mm/min such as sample 2, 3 and 4 showed an acceptable welding appearance and they appeared to be approximately the same despite the variation in the rotational speed and the tool temperature. This lowest travelling speed that combined with a set of higher rotational speed and tool temperature gave an adequate time to the materials to stir and soften together. In addition, sample 8 and 12 have a roughly the same surface appearance such as the pervious set of samples. They were joined at the highest rotational speed (1800 rpm) and tool temperature of 120 and 90 °C. These welding conditions also provide an adequate heat to stir and soften the two pieces together. The three samples 6, 11 and 16 have a relatively similar appearance and they were welded at the lowest welding temperature (50 °C). It is obvious that the surface of these samples was rather rough and this is due to the generated heat was not sufficient to make the semi-molten material flow easily under the shoulder.

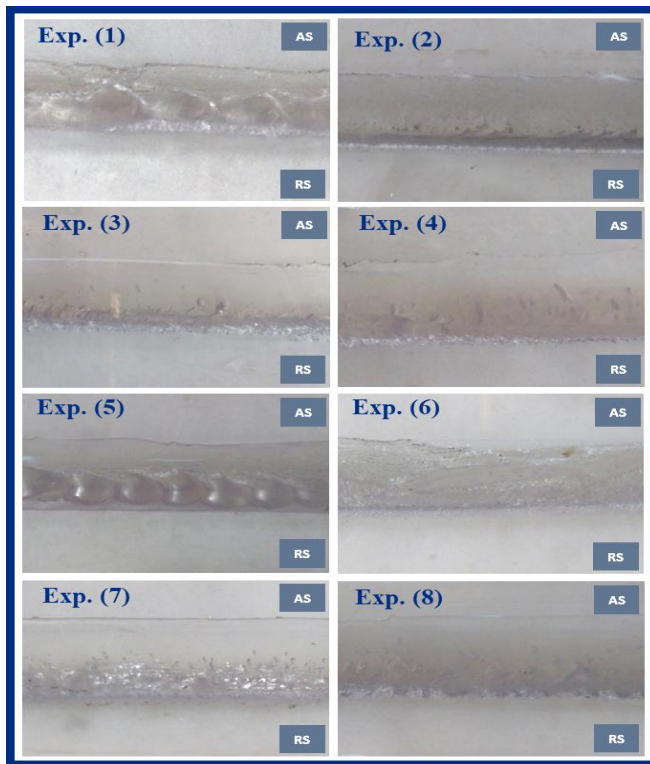


**Fig. 4** Enlarged views of welded plates made using parameters of experimental trials 1 to 8, showing the welding appearance.

This is due to the need for additional mechanical finishing operations such as milling or polishing to adjust the desired roughness, thickness or flatness. In order to achieve a good surface appearance, suitable process parameters should be selected. The surface appearance of the welded samples (each sample is composed of two sheets) is represented as shown in Fig. 4 and Fig. 5. The welding appearance varies according to the combination of the process parameters. The

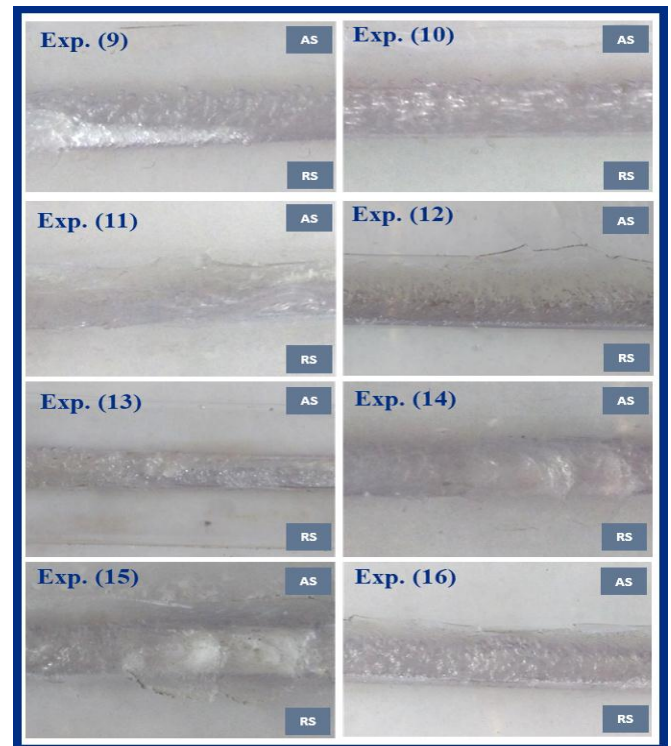


**Fig. 5** Enlarged views of welded plates made using parameters of experimental trials 9 to 16, showing the welding appearance.

However, the visual examination showed that the weld surface seems to be less rough with increasing the tool rotational speed. The specimens welded at high temperature (140°C) including specimen 7, 10 and 13 showed the shoulder boundary imprint on the surface of the welded plate and that is seen as damage to the surface appearance especially in specimen 13 which was welded at the highest welding speed (120 mm/min) and the lowest rotational speed (700 rpm).

**Table 4: Distribution of defects across the welded samples.**

Weld number		1	2	3	4	5	6	7	8	9	10	11	12	13	14	15	16	
Type of defect	Surface groove	•		•		•		•										
	Flash	•				•		•										
	voids						•	•	•	•	•	•	•	•	•	•	•	
	Tunnel	•												•		•		
	Island	•					•	•				•						
	Discontinuous bonding line		•	•	•								•					
	Macro-crack						•			•						•	•	•
	Root	•					•		•	•		•						

Finally, the sample 9, 14 and 15 showed inhomogeneous appearance along the welding line which composed of melted and non-melted regions.

**3.3 Defects in the welded square butt joints**

During the investigation of the different joint’s microstructure, several defects have been found in the welding nugget. The presence of these defects has a negative impact on the mechanical properties of the welded joints because they may act as an initial crack during loading or may reduce the thickness of the tested specimen, etc. The existence of these defects implies that the sample is welded outside the optimum welding parameters. Therefore, analysing these defects is essential to recognize the welding conditions that cause such defects; hence, the improper welding conditions could be excluded. The defects can be classified into the following types: root defects, surface grooves, flash formation, voids or cavities, tunnels, islands of melted and non-melted material, discontinuous bonding line and macro cracks. The distribution of these defects across the welded samples is shown in Table 4.

To make it easy to identify the position of the welding defects in the examined cross-section, the welding nugget can be divided into five main regions as shown in Fig. 6. The first and the second region are the areas where the advancing side and retracting side meet with the parent material, respectively. The third and the fourth regions are the top and bottom of the welding nugget, respectively. The fifth area is the central region which located in the middle of the welding nugget.

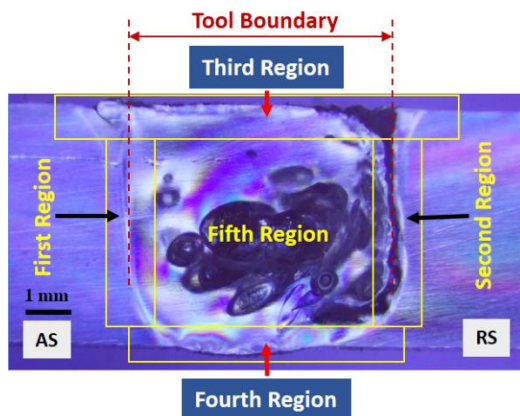


**Fig. 6 Macrograph of a cross-section of a welded sample (experimental trial 16), showing the main five regions in a typical PC weld nugget.**

**3.3.1 Islands of melted and non-melted material**

One of the defects that have been seen repeated in more than one sample is a defect that can be named as islands of melted and non-melted material. As the name implies, the island of melted material is formed by the accumulation of a pure melted material surrounded by lines or a series of spots of non-melted material as shown in Fig. 7. This island is located at the top of the welding nugget and also a part of it extended inside the central region. The common point between the samples experiences such a defect is the welding at a low processing temperature. As can be seen in Fig. 7 (a), the macrostructure of sample 1 showed a formation of the two kinds of islands.

The formation of these two large islands imply that the material is highly resist the deformation and microstructural changes. This imbalance in the material flow inside the welding nugget has been occurred as a result of combining low rotational speed (700 rpm) and low tool temperature (50 °C). The low external heat input by the tool cannot produce this lot of trouble in the welding nugget if the blend of the other two parameters is set at the right values which produce adequate heat as well as a sufficient material flow around the tool probe. When the spindle speed increased upto 1200 rpm and 1500, a much better flow with the absence of the non-melted island was observed as shown in Fig. 7 (b) and Fig. 7 (c), respectively.

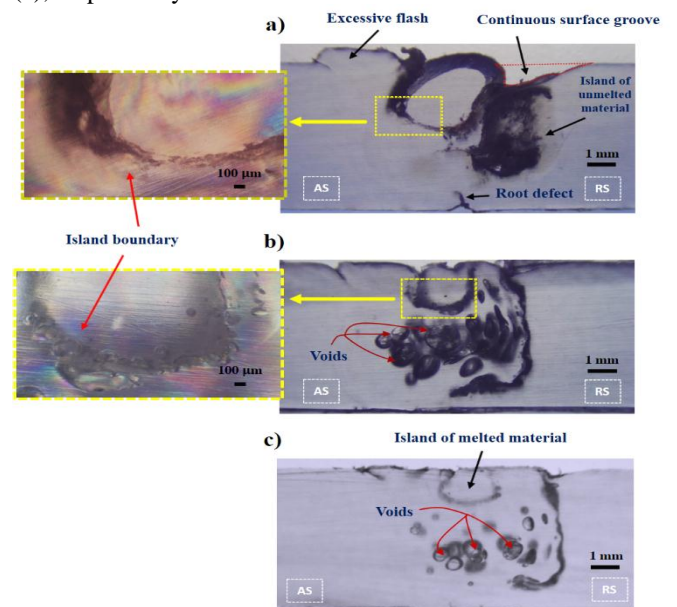


**Fig. 7 Macrographs of the stir zone of (a) Exp. (1), (b) Exp. (11) and (c) Exp. (6); alongside the magnification of the island boundary.**

### 3.3.2 Discontinuous bonding line and macro-cracks

Discontinuous bonding line and macro-crack are common types of defects that can be observed at the RS of the welded sample with FSW parameters not same as the optimum conditions as will be discussed later. As previously stated, the RS of a welding nugget is suffered from the lack of generated heat which responsible for the existence of such defects. The discontinuous bonding line is formed by spots or accumulations of non-melted material separated by tiny areas of melted materials as shown in Fig. 8. This type of defect is mainly seen in the samples welded at the lowest value of traverse speed (30 mm/min) and that includes samples 2,3 and 4. When the welding speed increases, the boundary of the RS could be transformed into a line of completely non-melted material with the formation of a macro-crack defect as shown in Fig. 9.

In addition, the formation of macro-crack defects in these samples was primarily occurred due to the low rotational speed (700 rpm) which produces an insufficient material flow around the FSW probe as shown in Fig. 9 (a) and Fig. 9 (b). Moreover, this type of defect can be formed as a result of cold-welding conditions as shown in Fig. 9 (c). Therefore, to reduce or to eliminate this defect the insufficient material flow as well as cold welding conditions should be eliminated.

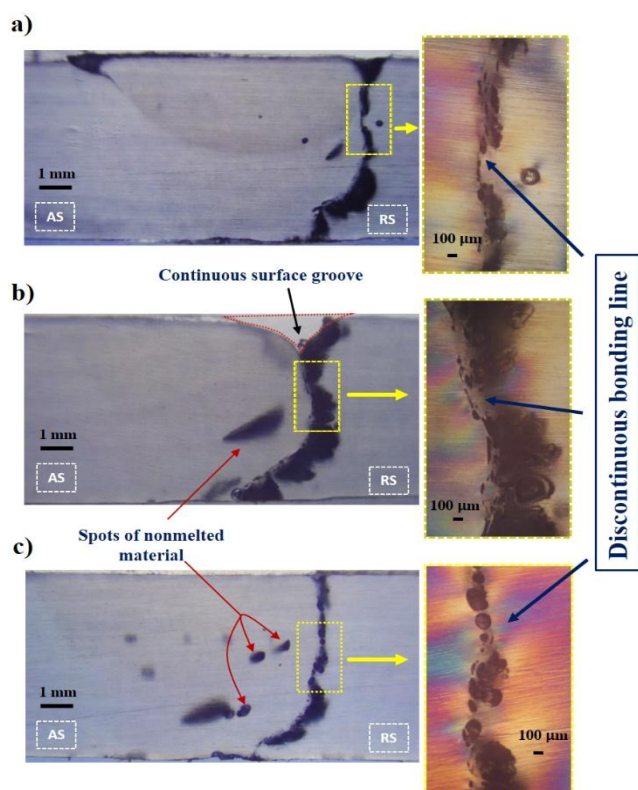


Fig. 8 Macrographs of the stir zone of (a) Exp. (2), (b) Exp. (3) and (c) Exp. (4); alongside the magnification of the discontinuous bonding line defect.

### 3.3.3 Tunnel defect

Tunnel defect is one of the most influential defects in the welded joint strength and it is different from a cavity or void in its size as well as its extension inside the welding seam. Tunnel defect is usually larger in size and always extends for a long distance inside the welding seam. This type of defect was observed in three different samples (sample 1, 13 and 15).

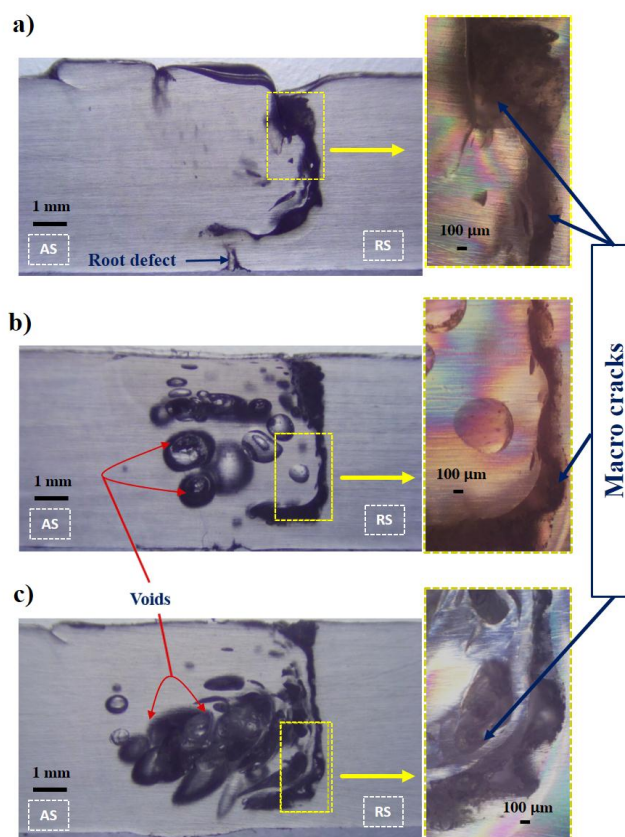


Fig. 9 Macrographs of the stir zone of (a) Exp. (5), (b) Exp. (9) and (c) Exp. (16); alongside the magnification of the macro-crack type defect.

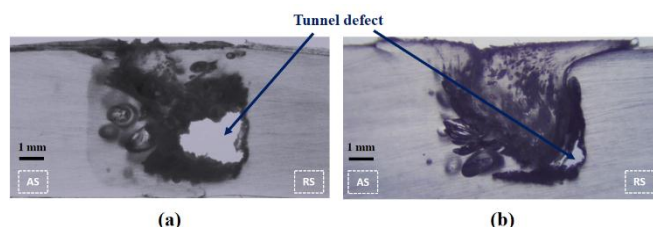


Fig. 10 Macrographs of the stir zone of (a) Exp. (13) and (b) Exp. (15).

In the case of sample 1, a small tunnel was found at the bottom of the non-melted island as a consequence of insufficient heat input. In the case of sample 13, a huge tunnel was formed at the bottom corner of the retreating side as a result of using one of the worst mixings of welding conditions as shown in Fig. 10 (a). This includes welding the two pieces at the highest value of welding speed (120 mm/min) and the lowest value of rotational speed (700 rpm). In this case, the material in front of the FSW tool was subjected to an enormous pushing force more than a stirring action. In the case of sample 15, a tunnel defect is also formed at the bottom corner of the retreating side as shown in Fig. 10 (b). This tunnel defect has a relatively small size compared to the previous one due to increasing the rotational speed to 1500 rpm which relatively improved the stirring action within the welded nugget.

### 3.3.4 Flash defects and surface grooves

The formation of flash on the top surface of the welding line usually leads to a surface groove defect and that can be noticed during the examination of sample 1,5 and 7. These

types of flaws can be easily seen by the naked eye through the inspection of the surface appearance of the welded plates. Formation of flash as well as surface groove can occur as a result of several reasons including using an improper tool design, machine-related error, operator error, and incorrect welding conditions. In case the tool design is the reason of such a defect, this is usually due to the shoulder rotating which is not the issue in this investigation since the shoulder was stationary.

However, the other three reasons are mainly related to the existence of an air gap between the upper surface of the welded plates and the lower surface of the shoulder. This air gap may be formed due to a certain amount of backlash existing in the assembly of the machine z-axis or the FSW tool assembly. Under certain welding conditions (cold-welding conditions) as in the case of samples 1 and 5, the axial pressure generated on the FSW tool by the material resistance, especially at the penetration state will push the FSW tool towards the upper direction leaving a small air gap which acts as a free space for the molten material to leak from. This gap could also be created due to an operator error during the setup stage. In this case of increasing the local temperature due to welding at a high value of rotational speed and tool temperature, the amount of molten polymer will increase. Therefore, this molten polymer will take the advantage of any air gap left due to an operator error or machine-related error to leak from. Figure 11 shows the stir zone of sample 7 which experiences a flash defect and surface groove.

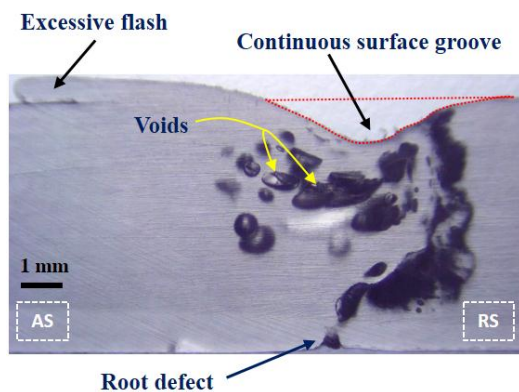


Fig. 11: Macrographs of the stir zone of Exp. (7).

### 3.3.5 Formation of voids

Under the presented welding conditions, the formation of voids or cavities has been found to be the most predominant defect in the welding nugget. To be more precise, 11 out of the 16 welded samples (about 70%) were found to suffer from the formation of the voids. The amount of voids and their size in the welding nugget are varying according to the welding conditions. In general, most of these voids was concentrated in the central region of the welding zone. The first group of samples (sample 1, 2, 3 and 4) which joined at the lowest value of traverse speed (30 mm/min) show very small amount of voids formation. This indicates that giving the two plastic plates an adequate time to stir together is the most significant factor to eliminate this type of defect. On the contrary, increasing the welding speed leads to increasing the number of voids as well as their size in most cases as shown in Fig. 12.

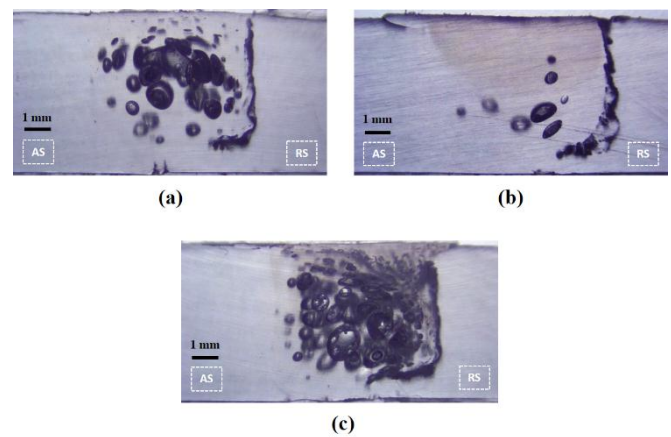


Fig. 12 Macrographs of the stir zone of (a) Exp. (8), (b) Exp. (10) and (c) Exp. (14).

### 3.3.6 Root defect

When a traditional FSW tool design (a tool with a rotary shoulder) or even a tool with a stationary shoulder is used, a small area at the bottom of the two matching plates (root region) is left without welding as a result of the insufficient tool penetration. This lack of penetration is one of the characteristics of the aforementioned tools. In other words, if the FSW probe penetrates the entire depth of the welded plates, the bottom surface of the FSW probe will come into contact with the backing plate which will cause some problems to the FSW probe and the backing plates. Firstly, if the backing plate is made of a harder material than the probe, the FSW probe will heat up and wear out. On the contrary, if the backing plate is made of a less hard material than the probe, the FSW probe will stir the backing plate with the material being welded. In order to solve this problem from the tool design perspective, a tool with a double-shoulder (bobbin tool) is used. This additional lower shoulder acts as a backing plate which allows the tool to penetrate through the entire material depth but the major drawback of this tool involves its inability to retract at any time during the welding process. This geometric drawback of the bobbin tool opens the way for the tools that perform single side welds to be widely used compared to the bobbin tools. Despite the single side tools cannot penetrate throughout the entire depth, a welding nugget with the absence of root defect can be obtained as shown in Fig. 13.

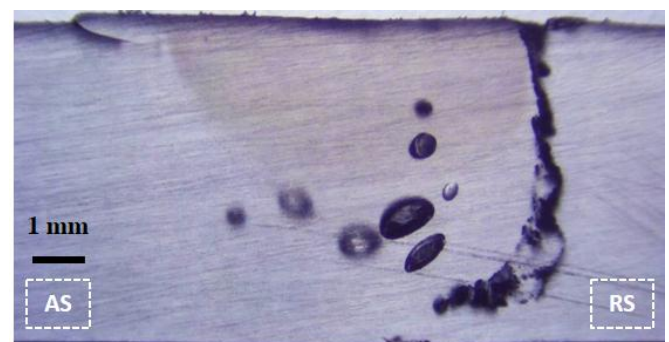
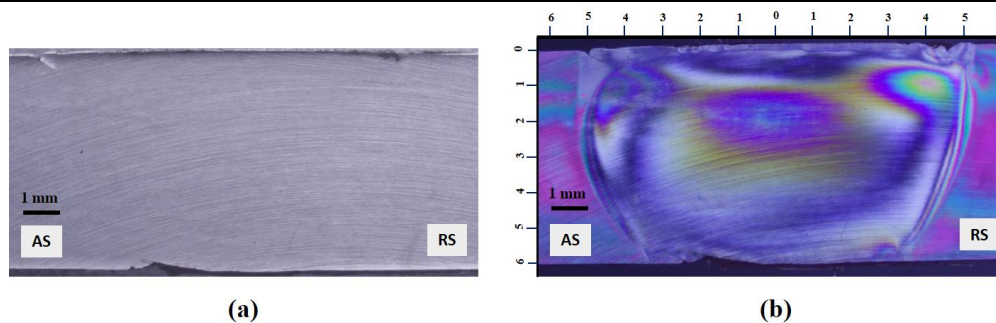


Fig. 13 Macrographs of the stir zone of Exp. (12).

**Table 5: Mechanical properties of each individual specimen.**

Extracted specimen	Flexural strength (MPa)	Joint efficiency (%)	Flexural modulus (MPa)	Flexural Offset Yield Strength
A	85.9	92.6	2172.6	62
B	87.3	94.1	2093.6	54
C	83.5	90	1995.8	56
Mean	85.6	92.2	2087.3	57.3



**Fig. 14: Macrographs of the stir zone of the sample welded at the optimum welding parameters; 1800 rpm rotational speed, 30 mm/min welding speed and 50 °C tool temperature using (a) ordinary optical microscope and (b) polarized light microscope.**

### 3.4 Producing of a nearly defect-free welded joint

The sample welded at the highest value of rotational speed (1800 rpm) and the lowest value of both welding speed (30 mm/min) and tool temperature (50 °C) achieved about 92.2% relative to flexural strength of the base material. This increase in the rotational speed (which increases the frictional heat to its maximum value) alongside the external heat input of the FSW pin (which heated the pin to its minimum value) were merged together to achieve an optimum value which produced a welding nugget is nearly similar to the base material as shown in Fig. 14 (a).

The flexural stress-strain curves of three extracted samples compared to the base material are represented as shown in Fig. 15. In addition, the flexural strength, flexural modulus and flexural offset yield strength of each individual specimen are represented in Table 5. When the welding is carried out at the highest rotational speed, the stirring action between the two plastic plates improved and sufficient flow of the material in the welding nugget is achieved. The low traverse speed of the pin along the welding seam is a key factor in order to make the combination of the two other factors work in the favor of improving the mechanical properties of the welded sample. Furthermore, this low traverse speed allowed the heat produced during welding to uniformly distributed at the advancing and the retreating side and that can be seen through the investigation of the heat affected zone (HAZ) of the welding nugget as shown in Fig. 14(b).

## 4 CONCLUSION

The aim of this work is to study the influence of probe temperature, spindle speed and welding speed on the formation of defects during friction stir welding of PC using a cylindrical threaded probe and a stationary shoulder. Based on the experimental results and discussion, the key findings could be summarized as follows:

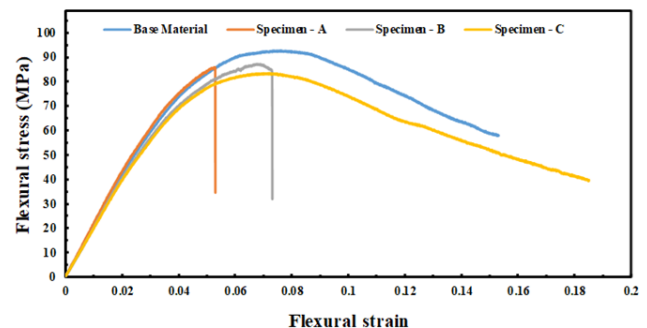


**Fig. 15 Flexural stress-strain curves of three samples extracted from the welded butt joint that made at the optimum welding parameters; 1800 rpm rotational speed, 30 mm/min welding speed and 50 °C tool temperature compared to the base material.**

- Formation of the discontinuous bonding line and macro-crack were a result of insufficient heat generation as well as lack of proper stirring on the retreating side.
- The macrostructure examination showed that welding speed has a positive relationship with the formation of voids inside the welding nugget.
- The formation of what looks like rope knots on the surface of some samples was a result of resisting the material in the welding nugget to flow due to welding at cold conditions: welding at the lowest value of rotational speed combined with low a tool temperature.
- The optimum welding conditions which achieved about 92.2% compared to the flexural strength was the rotational speed of 1800 rpm, welding speed of 30 mm/min and tool temperature of 50 °C.

- Welds with the higher flexural strength showed nearly a defect-free welding nugget with almost a symmetric HAZ in the advancing and retreating side.

#### ACKNOWLEDGMENT

The authors would like to thank the Science and Technology Development Fund (STDF)/Egypt for funding this work.

#### REFERENCES

1. Huang, Y., et al., *Friction stir welding/processing of polymers and polymer matrix composites*. Composites Part A: Applied Science and Manufacturing, 2018. **105**: p. 235-257.
2. Troughton, M.J., *Handbook of plastics joining: a practical guide*. 2008: William Andrew.
3. Amanat, N., N.L. James, and D.R. McKenzie, *Welding methods for joining thermoplastic polymers for the hermetic enclosure of medical devices*. Medical engineering & physics, 2010. **32**(7): p. 690-699.
4. Thomas, W.M., et al., *Friction welding*. 1995, Google Patents.
5. Shehabeldeen, T.A., et al., *A Novel Method for Predicting Tensile Strength of Friction Stir Welded AA6061 Aluminium Alloy Joints Based on Hybrid Random Vector Functional Link and Henry Gas Solubility Optimization*. IEEE Access, 2020. **8**: p. 79896-79907.
6. Mendes, N., et al., *Effect of friction stir welding parameters on morphology and strength of acrylonitrile butadiene styrene plate welds*. Materials & Design, 2014. **58**: p. 457-464.
7. Kumar, S. and B.S. Roy, *Friction Stir Welding of Glass Filled Nylon 6 Composites*. Materials Today: Proceedings, 2020. **24**: p. 754-762.
8. Nath, R.K., P. Maji, and J.D. Barma, *Effect of tool rotational speed on friction stir welding of polymer using self-heated tool*. Production Engineering, 2022: p. 1-8.
9. Sahu, S.K., et al., *Friction stir welding of polypropylene sheet*. Engineering science and technology, an international journal, 2018. **21**(2): p. 245-254.
10. Rehman, R.U., J. Sheikh-Ahmad, and S. Deveci, *Effect of preheating on joint quality in the friction stir welding of bimodal high density polyethylene*. The International Journal of Advanced Manufacturing Technology, 2021. **117**(1): p. 455-468.
11. Eslami, S., et al., *Polyethylene friction stir welding parameter optimization and temperature characterization*. The International Journal of Advanced Manufacturing Technology, 2018. **99**(1): p. 127-136.
12. Sheikh-Ahmad, J., et al., *Effect of process temperatures on material flow and weld quality in the friction stir welding of high density polyethylene*. Journal of Materials Research and Technology, 2022.
13. Omer, M.A., et al., *A review on friction stir welding of thermoplastic materials: recent advances and progress*. Welding in the World, 2021: p. 1-25.
14. ASTM, S., *Standard test methods for flexural properties of unreinforced and reinforced plastics and electrical insulating materials. ASTM D790*. Annual book of ASTM Standards, 1997.